*Anal. Chem.* **1996,** *68,* 1116−1123

# Quantitative in Situ Monitoring of an Elevated Temperature Reaction Using a Water-Cooled Mid-Infrared Fiber-Optic Probe

Paul MacLaurin* and Nicholas C. Crabb

*Process Technology Department, Zeneca FCMO, Leeds Road, Huddersfield HD2 1FF, U.K.*

Ian Wells and Paul J. Worsfold

*Department of Environmental Sciences, University of Plymouth, Drake Circus, Plymouth PL4 8AA, U.K.*

David Coombs

*Graseby Specac Limited, River House, 97 Cray Avenue, St. Mary Cray, Orpington BR5 4HE, U.K.*

**A novel water-cooled mid-infrared fiber-optic probe is described which is heatable to 230 °C. The probe has chalcogenide fibers and a ZnSe internal reflection element and is compact and fully flexible, allowing access to a wide range of standard laboratory reaction vessels and fume cupboard arrangements. Performance is demonstrated via the in situ analysis of an acid-catalyzed esterification reaction in toluene at 110 °C, and the results are compared with those from a conventional extractive sampling loop flow cell arrangement. Particular emphasis is given to the quantitative interpretation of the spectroscopic data, using gas chromatographic reference data. Calibration data are presented for univariate and partial least squares models, with an emphasis on procedures for improving the quality of interpreparation calibration and prediction through the use of focused reference analysis regimes. Subset univariate procedures are presented that yield relative errors of <5%, and bias-corrected partial least squares procedures are described that result in relative errors of interpreparation calibration and prediction consistently <3%. This paper demonstrates the considerable power of fiber-optic mid-IR spectroscopy combined with bias correction partial least squares procedures for the efficient in situ quantitative analysis of laboratory scale reactions.**

From its roots in commodity chemicals manufacturing, process analytical chemistry is now impacting on virtually all sectors of chemical processing. One example is the fine chemicals industry, where typically batch processing, often in a nondedicated plant, has required the development of a multifaceted approach to process analysis.[1] In addition to producing a diverse range of chemical entities, fine chemicals manufacturing generally involves the frequent introduction of new processes, which require extensive and time-consuming process research and development, and the desire for greater efficiency has led to the process analytical chemistry philosophy being applied during process development. On-line analysis of laboratory-scale reactions can markedly improve both the timeliness and quality of information regarding reaction mechanisms and kinetics, as compared with traditional approaches of extractive sampling and quenching followed by liquid chromatographic analysis. In contrast to on-plant process analyzers, the technology for on-line analysis in process development needs to be inherently versatile. Furthermore, analytical development times need to be kept to a minimum in order to maintain consistency with the time frame of process development programs. Mid-infrared spectroscopy is attracting increasing attention as a process analysis tool,[2] and this paper describes advances in the use of fiber-optic mid-IR spectroscopy for the in situ analysis of laboratory-scale organic reactions.

Vibrational spectroscopy has long been a powerful tool in materials characterization. Virtually all organic functional groups exhibit fundamental vibrations at frequencies in the mid-IR region of the electromagnetic spectrum (4000−400 $cm^{-1}$). Typically, the information content of mid-IR spectra is high, with bands that are often narrow and well resolved, allowing direct functional group assignment. IR absorbance spectra have traditionally been recorded using dispersive instruments, but since 1970, Fourier transform infrared (FT-IR) instruments have been available that are capable of collecting high-quality spectra in a fraction of the time previously required with enhanced signal-to-noise and wavenumber accuracy. Despite this speed of response and its potential to directly monitor functional group vibrations, FT-IR has found little application to date for the on-line analysis of organic reactions. This is largely attributable to underdeveloped sample interfacing.

Absorptions in the mid-IR region tend to be strong, necessitating the use of short path lengths for transmission studies. Attenuated total reflection (ATR) techniques provide a means of achieving path lengths of effectively only a few micrometers and as a result have become a general solution for liquid sample analysis.[3] ATR spectroscopy utilizes the absorbances that occur when total internal reflection takes place at the interface between two materials. If a transparent material of high refractive index

(1) Crabb, N. C.; McLennan, F. *Process Control Qual.* **1992**, *3*, 229−235.

(2) Crabb, N. C.; King, P. W. B. Molecular Spectroscopy. In *Process Analytical Chemistry*; McLennan, F., Kowalski, B. R., Eds.; Blackie: London, 1995.

(3) Harrick, N. J. *Internal Reflection Spectroscopy*; Wiley: New York, 1967.



0003-2700/96/0368-1116$12.00/0 

is placed in direct contact with the sample, light passing through this at angles above a critical angle will be reflected at the sample interface. In the process of reflection, an evanescent wave penetrates the sample medium, giving rise to partial absorption of the beam according to the vibrational frequencies of the sample.

The missing link, therefore, for in situ FT-IR analysis is a means of transmitting the radiation between the spectrometer and the internal reflection element. One option is the use of optical light guides, hollow conduits internally coated with a reflecting material such as nickel or gold.[4] "Light pipes" have been used in conjunction with ATR probes for reaction monitoring, but their versatility is hampered by their rigid construction. Alternatively, reaction vessels can be constructed with integral internal reflection elements in dedicated spectrometer systems, but again, these are somewhat restrictive.[5]

Process development activity tends to involve the use of a wide range of reactor designs and capacities, and to gain access to a significant proportion of these reactors, a flexible approach to in situ IR sampling is required, something that is now possible due to recent developments in fiber-optic technology. In the simplest terms, optical fibers are a medium for transmitting radiant power and consist of a core and cladding. Radiation traveling in the core is confined to the core by reflection with the cladding that has a lower index of refraction. Fiber links are now commonplace for applications in visible and near-IR spectroscopy, but their performance decreases markedly in the mid-IR because the vast majority of materials have fundamental absorptions in this region. This problem is exacerbated by the low throughput of available fibers, the inherently low energy of mid-IR sources, and the relative insensitivity of mid-IR detectors. Recently, however, chalcogenide fibers have become commercially available and are beginning to be used in this context.

Chalcogenide glasses are vitreous materials made from group IV metals As, Ge, and Sb, together with the chalcogen elements S, Se, and Te. Chalcogenide transmission is good over the range 4000−1000 $cm^{-1}$, apart from lattice vibrations and absorption due to hydrogen-containing impurities at 2250−2100 $cm^{-1}$, although high-attenuation characteristics have restricted their practical use to lengths of 2 m. Nevertheless, 10 m chalcogenide fibers have been reported[6] for environmental analysis over a restricted spectral range.

The analysis of elevated temperature reactions raises further issues, however. Low glass transition temperatures, in combination with low softening temperature cladding materials, have restricted the use of chalcogenide fibers to temperatures of ∼70 °C, thus rendering a significant proportion of typical process development reactions inaccessible. To address this shortcoming, a fully flexible fiber-optic probe heatable to temperatures up to 230 °C has recently been developed.

This paper describes the concept and construction of a novel water-cooled mid-IR fiber probe and its use in the monitoring of a laboratory-scale esterification reaction at 110 °C. The acid-catalyzed reaction of but-2-enoic acid and butan-2-ol was selected on account of its reaction temperature being greater than 70 °C,

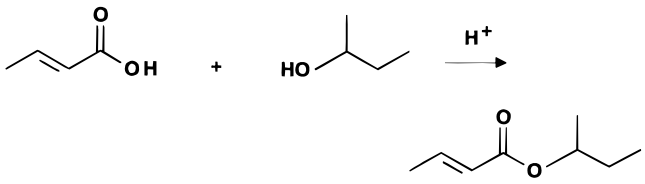


Figure 1. Acid-catalyzed reaction of but-2-enoic acid and butan-2-ol, to give the corresponding ester, *sec*-butyl but-2-enoate.

Table 1. Spectroscopic Variables for the Fiber Probe and Flow Cell Analysis

| accessory | spectral range, $cm^{-1}$ | spectral resoln, $cm^{-1}$ | *J*-stop, mm | *B*-stop, mm | gain | throughput, % |
|---|---|---|---|---|---|---|
| fiber probe | 4000−1000 | 4 | 11.00 | 15.00 | 2 | ∼13 |
| flow cell | 4000−700 | 4 | 11.00 | 8.00 | 1 | ∼48 |

apparent IR activity, and minimal safety hazards.[7] The reaction scheme is given in Figure 1. A series of three separate reactions was monitored using the fiber probe, and a further series of three reactions was monitored using an overhead ATR flow cell with a recirculating loop. Particular emphasis is given to the quantification of the reaction product (*sec*-butyl but-2-enoate) and the approach taken to improve its quantitative prediction with a minimum of analytical development.

## EXPERIMENTAL SECTION

**Instrumentation.** All spectra were recorded using a Perkin-Elmer System 2000 spectrometer fitted with a liquid nitrogen-cooled narrow band mercury−cadmium−telluride (MCT) detector. The spectrometer was operated in the infrared data manager (IRDM) environment using the time-resolved facility (TRIR). Spectra were stored as the mean of 64 co-added scans collected at 10 min intervals and were ratioed against an air background recorded immediately prior to analysis. The spectroscopic variables used for the fiber probe and the flow cell are summarized in Table 1.

The cooled mid-IR fiber probe consisted of two single-strand 750 $\mu$m, 1.5 m chalcogenide fibers with a numerical aperture of 0.4, in conjunction with a two-reflection 45° ZnSe internal reflection element (Figure 2a) and an adjustable optical interface for the spectrometer (Figure 2b). The composition of the fiber-optic material used was $As_{0.4}$, $Se_{0.2}$, $Te_{0.4}$, with minimal losses of 0.001 dB $m^{-1}$ at 6 $\mu$m. The glass transition temperature of this material was 136 °C, although the fibers do change their transmission characteristics at temperatures as low as 70 °C. The step index fibers were polymer clad and armor plated with spirally wound stainless steel, offering a bend radius of 15 cm. Larger diameter fibers could have been employed, enabling greater utilization of the available radiation, but this would have restricted the system flexibility. The fiber was deliberately overfilled in both numerical aperture and area, and a high-quality optical design was used to image the radiation back to the fiber. The probe features an integral internal water cooling system that maintains the fiber at 35 °C when the probe is immersed in a sample at 200 °C. Clearly, this is a safe margin with respect to the 70 °C fiber transition temperature. Cooling water was circulated via stainless steel

(4) Doyle, W. M.; Jennings, N. A. *Spectrosc. Int.* **1991**, *2*, 48−52.
(5) Full, A. P.; Puig, J. E.; Gron, L. U.; Kaler, E. W.; Minter, J. R.; Mourey, T. H.; Texter, J. *Macromolecules* **1992**, *25*, 5157−5164.
(6) Ewing, K. J.; Bilodeau, T.; Nau, G.; Aggarawal, I. D.; King, T.; Clark, R.; Robitille, G. Air and Waste Management/SPIE Conference Proceedings, McLean, VA, November 1994.
(7) Harwood, L. M.; Moody, C. J. *Experimental Organic Chemistry*; Blackwell: Oxford, 1989; pp 445−446.

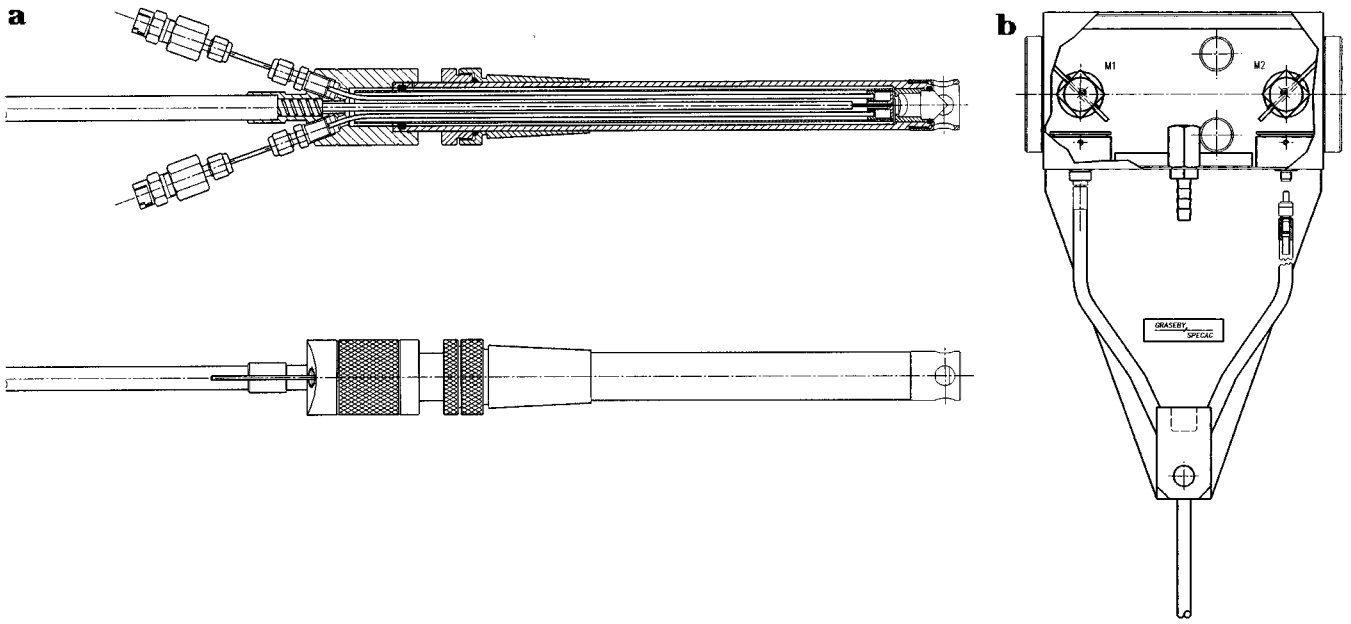


Figure 2. (a) Diagram of the water-cooled fiber probe illustrating the internal optics and cooling hardware. (b) Diagram of the instrument optical interface (plan view).

capillaries parallel to, but not in direct contact with, the fibers. The capillaries were housed in an air-filled tube surrounded by an insulating polymeric material. The probe was constructed from 316 stainless steel and was 256 mm long. The maximum diameter of the immersed probe head was 21 mm, but this could be reduced to 19 mm by detaching the removable ATR crystal protector. The probe was fitted with a stainless steel cone (B24/29) to provide a direct coupling for general laboratory glassware. The cone could be moved along the probe body and locked to vary the depth of immersion. The spectrometer interface consisted of an adjustable mirror and ZnSe lens arrangement for both the launch and collection optics. The cooling system was fitted to a standard laboratory tap via a 50 $\mu$m filtering device, and cooling water was supplied at a rate of 15−20 mL min$^{-1}$.

All flow cell data were collected using a Graseby Specac advanced overhead ATR system fitted with a 550 $\mu$L thermostabilized flow-through top plate assembly, incorporating a six-reflection 45° ZnSe internal reflection element and Kalrez gaskets. The flow cell was maintained at 90 °C throughout all experiments. The reaction mixture was continuously recirculated from the reaction vessel through narrow bore stainless steel tubing via a Gilson Minipuls 3 peristaltic pump fitted with Viton rubber pump tubing.

Gas chromatography (GC) was carried out using a Hewlett Packard HP 5890 Series II chromatograph with a 25 m Chrompack Cp-Sil-5CB 0.32 mm i.d. capillary column.

**Procedure.** All reactions were carried out in a standard 1 L flanged reaction vessel fitted with a stirrer, Dean−Stark apparatus, thermometer, and either the fiber probe or a stainless steel sampling tube for the flow cell experiments. Heat was supplied via a heating mantle. The experimental setup for the fiber probe experiments (preparations 1−3) is illustrated schematically in Figure 3. The setup for the flow cell experiments (preparations 4−6) was identical except for the use of the stainless steel tubing and pump arrangement in place of the fiber probe.

At room temperature, ~86 g of 98% but-2-enoic acid (Aldrich) was added to 500 mL of toluene (Fisons) with stirring, followed by the addition of 154 mL of butan-2-ol (Aldrich). At $t = 0$ min, 2 mL of sulfuric acid (Fisons) was added, and the reaction mixture was heated to 110 °C. Reflux at this temperature was maintained throughout the course of the 8 h reaction.

A sample was manually extracted at $t = 0$ min and at 30 min intervals thereafter for 8 h. The samples were used for reference analysis by an internal standard gas chromatography procedure for the quantification of but-2-enoic acid, butan-2-ol, and *sec*-butyl but-2-enoate. The procedure used split injection and temperature programming with undecane as internal standard. Sample solutions were prepared by the dilution of ~1.0 g of accurately weighed reaction mixture to 100 mL with dichloromethane. All samples solutions were analyzed in duplicate, and a standard mixture was analyzed after every four injections.

**Chemometric Data Analysis.** *General Multivariate Calibration.* Partial least squares (PLS) regression models were developed for all constituents using the spectra from the six individual preparations and the GC reference data. All models were developed using the PLS-1 algorithm of the Perkin-Elmer Quant+ software. Full cross validation was used for all calibrations. Model dimensionality was determined as the first significant local minimum in the relative root mean square error of cross validation:

$$\text{RRMSECV (\%)} = \frac{100}{\bar{y}}\sqrt{\frac{\sum_{i=1}^{I}(y_i - \hat{y}_i)^2}{I}}$$

where $y_i$ is the concentration of object $i$, $\hat{y}_i$ is the predicted concentration of object $i$, $I$ is the total number of objects used in the calibration, and $\bar{y}$ is the mean analyte concentration. Because the prediction objects are not used during calibration, no degrees of freedom are lost.

*Interpreparation Calibration and Prediction.* The aim of this exercise was not to develop a universal calibration for the long-term determination of *sec*-butyl but-2-enoate in the reaction mixture, because this would require extensive additional experimental preparations, supplemented by full reference analysis by

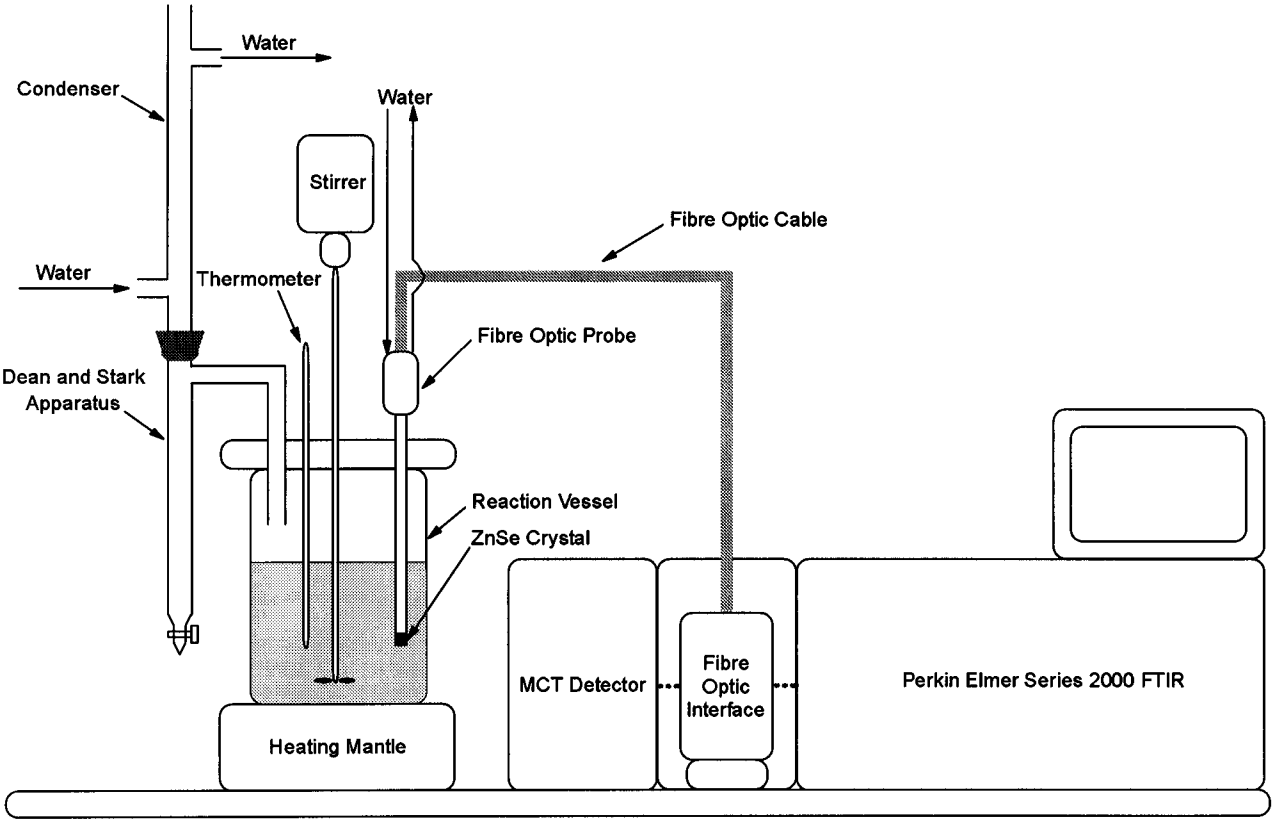


Figure 3. Experimental setup for the in situ analysis of the preparation of *sec*-butyl but-2-enoate using the water-cooled fiber probe.

gas chromatography. Such an approach to quantitation is in itself time-consuming, but this would also lead to significant delays in the process development program. Instead, procedures for extracting the maximum information about individual preparations with minimal reference analysis were investigated, with emphasis on the determination of the reaction product *sec*-butyl but-2-enoate.

Quantitation of *sec*-butyl but-2-enoate was carried out using univariate and multivariate calibration procedures, again using PLS-1 with full cross validation for all the multivariate models. For both univariate and multivariate procedures, the quality of the calibration models was compared in terms of their abilities to predict the concentration of *sec*-butyl but-2-enoate in other preparations and was quantified by the relative root mean square error of prediction (RRMSEP). The RRMSEP is calculated in the same way as the RRMSECV and is expressed as a percentage. Again, no degrees of freedom are lost because all the prediction samples are independent of the calibration model.

Two calibration and prediction regimes were investigated, and they are summarized below.

*(i) Single Preparation Calibration.* Calibration models (univariate and PLS) were developed using the spectra from a single preparation with full GC reference data. These models were used to predict the concentration of *sec*-butyl but-2-enoate in the other preparations from the spectra recorded using the same sampling accessory.

*(ii) Bias Correction and Subset Calibration.* PLS models were developed using the spectra from a single preparation with full GC reference data, as for the single preparation calibration scenario. However, prior to the prediction of the ester concentration in subsequent preparations, GC reference data and the appropriate spectra for four samples from the preparation under investigation were made available. This enabled an estimate to be made of the measurement bias between the original calibration and the preparation under investigation. The significance of the bias was estimated using *F*-statistics and applied accordingly as either an offset correction or a slope and offset correction. Bias correction does not change the original PLS model, i.e. the original latent variables are retained; only the newly predicted values are corrected for the bias. It should be noted that applying bias correction to interpreparation calibration and prediction represents a departure from its conventional use. Bias correction is generally used to correct for systematic differences caused by changing a sampling accessory or transferring a calibration between instruments. However, the nature of the data manipulation is very similar, and the concept holds, providing that good-quality reference data are available.

Applying the same principle to univariate statistics leads to subset calibration. Unlike PLS, the determination of a least squares univariate regression equation does not involve data reduction. It follows, therefore, that bias correction is not necessary because the same four samples used for PLS bias correction can be directly used with their reference data to determine a new univariate regression equation. This equation can then be used for intrapreparation prediction of the *sec*-butyl but-2-enoate concentrations from the other spectral data collected in that preparation.

## RESULTS AND DISCUSSION

The reaction profile of preparation 1, as determined by gas chromatography, is presented in Figure 4. As anticipated, it clearly shows the parallel consumption of but-2-enoic acid and butan-2-ol in tandem with the formation of *sec*-butyl but-2-enoate. Very similar profiles were observed for the other preparations.

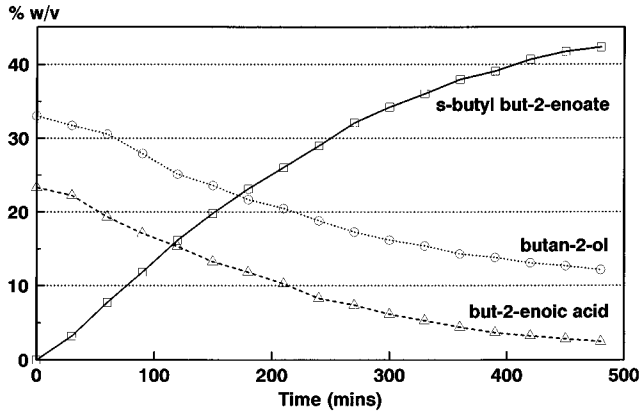


Figure 4. Reaction profile (preparation 1) determined by gas chromatography.

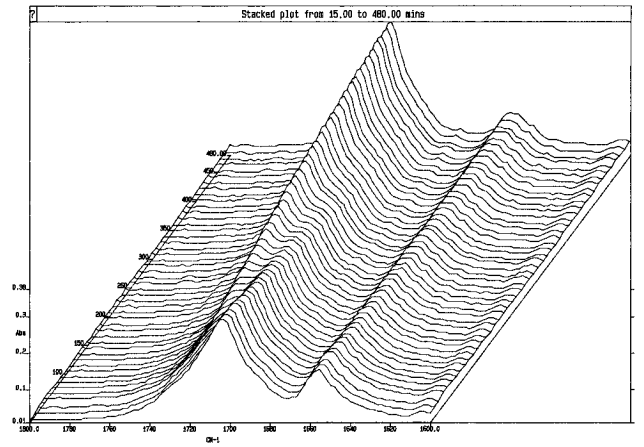


Figure 5. Time-resolved spectra of the carbonyl stretching region (preparation 1; fiber probe).

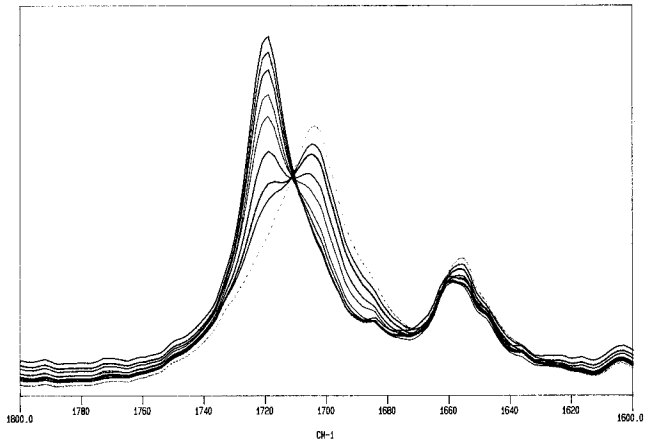


Figure 6. Spectral overlay of the carbonyl stretching region (preparation 1; fiber probe).

Figure 5 shows the high-quality time-resolved spectra of the carbonyl stretching region, collected during preparation 1 using the fiber probe. In accordance with the consumption of but-2-enoic acid and concurrent formation of *sec*-butyl but-2-enoate, the absorbance at 1700 $cm^{-1}$ ($\nu_S C{=}O$, $\alpha,\beta$-unsaturated carboxylic acid) clearly decreases as the band at 1720 $cm^{-1}$ ($\nu_S C{=}O$, $\alpha,\beta$-unsaturated ester) evolves. Overlaying a series of spectra taken at 30 min intervals during preparation 1 (Figure 6) illustrates this transition more clearly and verifies the high resolution achievable with liquid phase mid-IR spectroscopy. A spectral overlay of the C—O stretching region, again from preparation 1, is shown in Figure 7. Here, the development of the multiple C—O stretching bands associated with the formation of the $\alpha,\beta$-unsaturated ester are clearly visible ($\nu_{AS}C{-}C(=O){-}O$, 1265 $cm^{-1}$ and 1185 $cm^{-1}$; $\nu_{AS}O{-}C{-}C$, 1100 $cm^{-1}$).

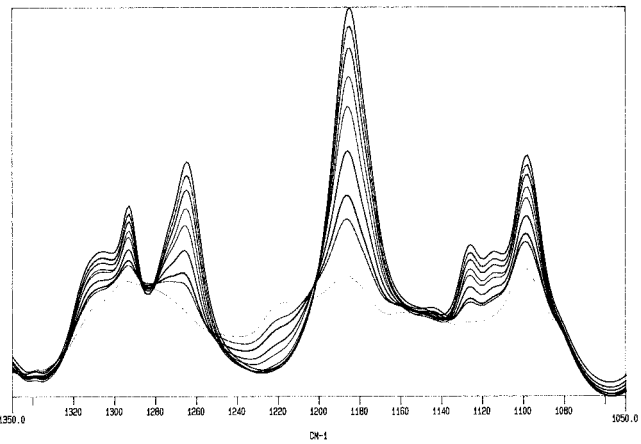


Figure 7. Spectral overlay of the C—O stretching region (preparation 1; fiber probe).

Table 2. PLS-1 Full Cross Validation Models for All Constituents after Mean-Center Scaling

| accessory | analyte | data set | no. of objects | optimal dimensionality | RRMS CV, % |
|---|---|---|---|---|---|
| fiber-optic probe | *sec*-butyl but-2-enoate | 1 | 16 | 2 | 1.54 |
| | | 2 | 16 | 2 | 2.36 |
| | | 3 | 16 | 2 | 1.70 |
| | butan-2-ol | 1 | 16 | 2 | 2.19 |
| | | 2 | 16 | 2 | 3.28 |
| | | 3 | 16 | 2 | 1.87 |
| | but-2-enoic acid | 1 | 16 | 2 | 3.53 |
| | | 2 | 16 | 2 | 5.49 |
| | | 3 | 16 | 2 | 4.35 |
| flow cell | *sec*-butyl but-2-enoate | 4 | 15 | 2 | 2.52 |
| | | 5 | 10 | 2 | 2.43 |
| | | 6 | 14 | 2 | 2.16 |
| | butan-2-ol | 4 | 15 | 2 | 2.64 |
| | | 5 | 10 | 1 | 1.76 |
| | | 6 | 14 | 2 | 2.67 |
| | but-2-enoic acid | 4 | 15 | 2 | 5.58 |
| | | 5 | 10 | 1 | 3.05 |
| | | 6 | 14 | 2 | 4.26 |

**General Multivariate Calibration.** Details of the PLS-1 full cross validation models developed with the data from the six individual preparations is presented in Table 2. Preliminary modeling indicated that most of the correlated spectral variance was in the spectral region 2000−1000 $cm^{-1}$, and all models were therefore developed using this range. Various approaches to spectral preprocessing were considered, but only mean-center scaling had a beneficial impact on the RRMSECV. Model dimensionality was generally estimated at 2, returning RRMSECV values of less than 5% in all but two cases.

Figure 8 shows the coefficient weightings plot for *sec*-butyl but-2-enoate from the preparation 1 data set. The areas of correlation are consistent with those of high spectral variance identified in Figures 5−7, i.e., the C=O and C—O stretching regions. Similar correlation patterns were observed for the *sec*-butyl but-2-enoate models for the data from the other preparations. It is interesting to note the negative peak at 1700 $cm^{-1}$, consistent with acid consumption, next to the large positive peak at 1720 $cm^{-1}$, consistent with ester formation. Examination of the coefficient

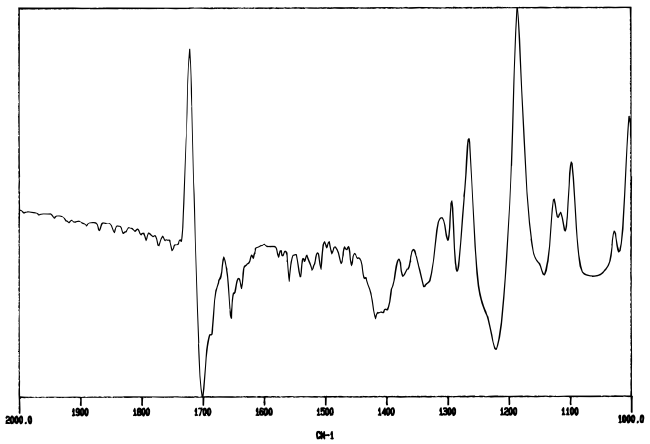


Figure 8. PLS-1 coefficient weightings plot for *sec*-butyl but-2-enoate model from preparation 1.

Table 3. PLS-1 Full Cross Validation Models of the Combined Data Sets After Mean-Center Scaling

| accessory | analyte | no. of objects | optimal dimensionality | RRMSECV, % |
|---|---|---|---|---|
| fiber-optic probe | *sec*-butyl but-2-enoate | 48 | 3 | 2.26 |
| | butan-2-ol | 48 | 3 | 3.18 |
| | but-2-enoic acid | 48 | 3 | 5.18 |
| flow cell | *sec*-butyl but-2-enoate | 39 | 2 | 18.83 |
| | butan-2-ol | 39 | 2 | 13.08 |
| | but-2-enoic acid | 39 | 2 | 21.05 |

weightings for butan-2-ol and but-2-enoic acid revealed a very similar correlation structure but in mirror image to that for the *sec*-butyl but-2-enoate. This is rationalized by the fact that there is no mechanism for controlling the calibration design during reaction monitoring; as the acid and alcohol are consumed, the ester is produced concurrently, and therefore no discrimination can be made in terms of covariance.

In addition, all of the data obtained from the fiber probe were combined to form a larger data set for calibration, as were all of the flow cell data. The resulting model details are presented in Table 3. It can be seen that the models for all constituents developed from the fiber probe data yielded relative errors of the same magnitude as the individual preparation models (Table 2) but that a third dimension was required to model the interpreparation variance. However, the relative errors of the flow cell models were significantly higher (>20% for the but-2-enoic acid), and examination of the model parameters revealed significant differences between the spectral data sets. The scores of the first two latent variables revealed three distinct groupings according to the individual preparation (4−6), although the GC reaction profiles were very similar. This was explained by differences in the background measurements collected prior to each preparation.

**Interpreparation Calibration and Prediction.** *Single Preparation Calibration.* Resolution in the mid-IR allows the direct selection of frequencies for univariate calibration. Preliminary investigations indicated that the C−O stretching region was more stable than the carbonyl region, and the absorbance at 1185 $cm^{-1}$ ($\nu_{AS}$C−C(=O)−O) was therefore used for calibration. The absorbance at 1055 $cm^{-1}$ was subtracted from this to account for temporal drift in the background spectrum.

Table 4. Univariate Calibrations and Predictions for *sec*-Butyl But-2-enoate (Single Preparation Calibration)

| accessory | calibrn set | slope | intercept | correln coeff | predn set | RRMSEP, % |
|---|---|---|---|---|---|---|
| fiber-optic probe | 1 | 0.006 57 | 0.0911 | 0.9966 | 2 | 2.86 |
| | | | | | 3 | 7.61 |
| | 2 | 0.006 38 | 0.0931 | 0.9882 | 1 | 3.53 |
| | | | | | 3 | 8.93 |
| | 3 | 0.006 00 | 0.1176 | 0.9976 | 1 | 8.25 |
| | | | | | 2 | 9.32 |
| | 4 | 0.020 94 | 0.2331 | 0.9983 | 5 | 53.86 |
| | | | | | 6 | 5.89 |
| flow cell | 5 | 0.016 35 | 0.5610 | 0.9978 | 4 | 48.71 |
| | | | | | 6 | 44.24 |
| | 6 | 0.019 54 | 0.2921 | 0.9976 | 4 | 6.06 |
| | | | | | 5 | 9.32 |

Table 5. PLS-1 Predictions for *sec*-Butyl But-2-enoate (Single Preparation Calibration)

| accessory | calibrn set | predn set | RRMSEP, % |
|---|---|---|---|
| fiber-optic probe | 1 | 2 | 6.19 |
| | | 3 | 5.22 |
| | 2 | 1 | 5.24 |
| | | 3 | 13.69 |
| | 3 | 1 | 13.93 |
| | | 2 | 21.11 |
| flow cell | 4 | 5 | 42.76 |
| | | 6 | 43.00 |
| | 5 | 4 | 48.99 |
| | | 6 | 136.0 |
| | 6 | 4 | 4.73 |
| | | 5 | 58.67 |

Calibration data are presented in Table 4, together with the relative errors of prediction for the other preparations. The slope and intercept values are quite similar for the three fiber probe models, and they yield RRMSEP values that are consistently <10% for the other preparations. The variability of the slope and intercept values for the univariate flow cell models is consistent with the background differences described above. These differences have manifested in gross errors in the prediction of other preparations, e.g., a relative error of 54% using the preparation 4 model to predict preparation 5.

The results of interpreparation predictions based on the PLS models from Table 2 are presented in Table 5. This again reveals large relative errors for the flow cell preparation data sets, but the fiber probe preparation models also resulted in prediction errors of up to 21%.

While some of the univariate interpreparation calibration and prediction results are quite encouraging, the general standard of prediction is rather poor, and in the context of a process development/process optimization excercise, predictions with relative errors of 40−50% are of little diagnostic value.

*Bias Correction and Subset Calibration.* Univariate subset calibrations were undertaken using four selected samples from each preparation. For preparations 1−4 and 6, the samples taken at $t$ = 60, 180, 300, and 420 min were used. The samples taken at $t$ = 60, 150, 240, and 330 min were used from preparation 5. Calibration details and prediction errors for each preparation are presented in Table 6. The univariate subset approach to intrapreparation calibration and prediction has resulted in relative errors of <3% for the fiber probe data and <5% for the flow cell data. This represents a marked improvement on the values of

Table 6. Univariate Subset Intrapreparation Calibrations and Predictions for *sec*-Butyl But-2-enoate

| accessory | calibrn set | slope | intercept | correln coeff | RRMSEP, % |
|---|---|---|---|---|---|
| fiber-optic probe | 1 | 0.00625 | 0.0925 | 0.9971 | 2.59 |
| | 2 | 0.00643 | 0.0912 | 0.9971 | 1.89 |
| | 3 | 0.00598 | 0.1184 | 0.9976 | 2.36 |
| flow cell | 4 | 0.02188 | 0.2162 | 0.9986 | 3.60 |
| | 5 | 0.01606 | 0.5634 | 0.9968 | 3.64 |
| | 6 | 0.01860 | 0.3068 | 0.9990 | 4.58 |

Table 7. Interpreparation Bias-Corrected PLS-1 *sec*-Butyl But-2-enoate Predictions

| accessory | calibrn set | predn set | bias corrn applied | RRMSEP, % |
|---|---|---|---|---|
| fiber-optic probe | 1 | 2 | offset | 1.71 |
| | | 3 | offset | 1.68 |
| | 2 | 1 | slope, offset | 1.19 |
| | | 3 | offset | 2.27 |
| | 3 | 1 | slope, offset | 1.25 |
| | | 2 | offset | 1.78 |
| flow cell | 4 | 5 | slope, offset | 2.00 |
| | | 6 | slope, offset | 2.41 |
| | 5 | 4 | slope, offset | 3.84 |
| | | 6 | offset | 3.52 |
| | 6 | 4 | none | 4.73 |
| | | 5 | slope, offset | 2.67 |

10% and up to 54%, respectively, from the single preparation calibration scenario, which were caused by variability in the regression equation coefficients. Any such systematic interpreparation variability will clearly have no effect on the predictive ability of subset intrapreparation calibration and predictions.

The same four samples from each preparation were also used to determine the bias correction for the PLS models. The corrections used and the prediction results are given in Table 7. For all but one of the prediction sets, either an offset or a combined slope and offset correction was shown to have a significant impact on the relative errors, reducing the RRMSEP values to a mean of 1.6% for the fiber probe preparations and a mean of 3.2% for the flow cell preparations. As with the univariate subset predictions, this represents a significant improvement on the gross errors recorded using PLS calibration under the single preparation calibration scenario.

Both the univariate subset and PLS bias correction approaches to interpreparation calibration and prediction have proved beneficial in terms of the relative error of prediction under these conditions for this series of reactions. Furthermore, this has been possible with a minimum of reference analysis and is therefore consistent with process development activity.

**Benefits for Process Development.** In this particular application, the characteristic mid-IR bands of the ester provided stable and well-resolved bands, allowing direct quantification by the univariate procedures discussed above. However, such an approach is unlikely to be appropriate for data from analytical systems of lower resolution, such as UV−visible and near-IR spectroscopy and electrochemical sensing devices. Moreover, univariate procedures will not be adequate for interpreparation calibration and prediction for applications in mid-IR spectroscopy, where the spectral transitions are subtle or the bands are subject to mutual interferences. In such cases, the numerical selectivity offered by reduced dimension multivariate calibration will be required for accurate predictions. This is supported by the *sec*-butyl but-2-enoate prediction results, which reveal that the bias correction PLS procedures have accommodated the interpreparation variability more comfortably than the univariate routines.

In the context of a process development environment, the concept of bias correction PLS procedures for interpreparation calibration and prediction is very powerful. A typical process development program will involve multiple reactions, often with only subtle differences in the conditions of these reactions. With full reference analysis of the first preparation in such a program, and the development of an appropriate PLS model for the constituents of interest, a limited but well-focused regime of reference analysis of the subsequent preparations will be sufficient to provide fully quantitative information from in situ IR spectra through the bias correction PLS procedure. Furthermore, there is potential to extend this concept to series of reactions with more radical differences in the reaction conditions, e.g., different catalysts. It is envisaged that judicious editing of mid-IR spectra will enable the influence of these differences to be marginalized, while the combined resolving power of mid-IR spectroscopy and bias correction PLS regression provides a robust quantification of the analytes of interest.

The adoption of these procedures goes a long way toward improving both the quality and timeliness of analytical measurements during process development. Ultimately, however, procedures capable of providing accurate information without the need for reference analysis are desired, and recent advances in the application of multivariate curve resolution techniques[8] show great promise. Since the need for reference analysis is eliminated, no secondary method development is required, and the potential hazards of extractive sampling are avoided. However, curve resolution procedures are far from trivial to implement successfully, and until more robust approaches are available, bias correction PLS provides an attractive alternative.

## CONCLUSIONS

Chalcogenide fibers have been shown to provide a safe and flexible approach to mid-IR sampling. The incorporation of a water cooling circuit in the body of a novel fiber probe has rendered this technology amenable to elevated temperature reactions which were previously not possible due to the instability of transmission properties above 70 °C.

Fiber probe analysis of the esterification of but-2-enoic acid and butan-2-ol at 110 °C produced high-quality mid-IR ATR spectra exhibiting well-resolved spectral features, confirming the high spectral resolution achievable with liquid phase mid-IR spectroscopy. The resulting spectra were as good as those obtained using a conventional flow-through overhead ATR arrangement with an extractive sampling loop but had the advantage of being truly in situ measurements.

Calibrations were developed using data from individual preparations from both the fiber probe and flow cell experiments, but they failed to predict the concentration of *sec*-butyl but-2-enoate in independent preparations without a high degree of error. To minimize these differences, procedures were investigated to provide accurate predictions with minimal time-consuming reference analysis. Using only four reference samples, subset intra-

(8) Tauler, R.; Kowalski, B. R.; Fleming, S. *Anal. Chem.* **1993**, *65*, 2040−2047.

preparation univariate calibration and prediction reduced the relative errors prediction to <3% for the fiber probe data sets and <5% for the flow cell data sets. Combinations of offset and slope corrections to the PLS models, determined using the same four reference samples, reduced the relative errors of interpreparation calibration and prediction to the order of 2% and 3% for fiber probe and flow cell data preparations, respectively.

## ACKNOWLEDGMENT

The authors acknowledge the assistance of L. L. Day and G. Poulter (Graseby-Specac) with the optics and J. N. Hirst (Zeneca FCMO) with the gas chromatography. Zeneca FCMO is gratefully acknowledged for financial support. I.W. thanks the SERC (U.K.) for a research studentship.

Received for review March 27, 1995. Accepted July 11, 1995.[⊗]

AC9502965

[⊗] Abstract published in *Advance ACS Abstracts,* January 1, 1996.